defects might be revealing in this regard.

Conclusions

Thin-film, bulk crystallization of sPP was shown to produce rectangular lamellar crystals with a unit-cell structure different from that originally proposed from doubly oriented samples. The new unit cell involves the presence of both left- and right-handed helices, consistent with the $(t_2g_2)_2$ conformation of sPP, whereas the existing unit cell was based implicitly upon helices of a *single* hand. In most crystals, the different packing schemes coexist, giving rise to a specific structural disorder of magnitude $b/2$. The two packing schemes depend upon the identical or opposite hand of crystallizing helices in relation to those on the crystal growth face. In addition, sheets on each (200) plane can also contain helices of opposite hand, which introduces a doubling of the b axis and necessitates the newly observed intersheet packing scheme.

Registry No. sPP, 26063-22-9.

References and Notes

(1) Permanent address: Institut Charles Sadron (CRM-EAHP), CNRS-ULP, 6, rue Boussingault, Strasbourg, France.
(2) Corradini, P.; Natta, G.; Ganis, P.; Temussi, P. A. *J. Polym. Sci., Part C* **1967**, *16*, 2477.
(3) Bunn, A.; Cudby, E. A.; Harris, R. K.; Packer, K. J.; Say, B. J. *J. Chem. Soc., Chem. Commun.* **1981**, 15.
(4) Marchetti, A.; Martuscelli, E. *J. Polym. Sci., Polym. Phys. Ed.* **1974**, *12*, 1649.
(5) Boor, J., Jr.; Youngman, E. A. *J. Polym. Sci., Polym. Chem. Ed.* **1966**, *4*, 1861.
(6) Boor, J., Jr.; *Ziegler-Natta Catalysts and Polymerizations*, Academic: New York, 1979; pp 117–122, 411.
(7) Zambelli, A.; Gatti, G. *Macromolecules* **1978**, *11*, 485.
(8) Schilling, F. C.; Tonelli, A. E. *Macromolecules* **1980**, *13*, 270.
(9) Bachmann, M. A.; Lando, J. B. *Macromolecules* **1981**, *14*, 40.
(10) Bachmann, M. A.; Gordon, W. L.; Weinhold, S.; Lando, J. B. *J. Appl. Phys.* **1980**, *51*, 5095.
(11) Weinhold, S.; Litt, M. H.; Lando, J. B. *J. Polym. Sci., Polym. Phys. Ed.* **1982**, *20*, 535.
(12) Lotz, B.; Wittman, J. C. *J. Polym. Sci., Polym. Phys. Ed.* **1986**, *24*, 1541.
(13) Khoury, F. *J. Res. Natl. Bur. Stand., Sect. A* **1966**, *70A*, 29.
(14) Padden, F. J., Jr.; Keith, H. D.; J. *Appl. Phys.* **1966**, *37*, 4013.
(15) Ogawa, T.; Elias, H.-G. *J. Macromol. Sci., Chem.* **1982**, *A17*, 727.
(16) Zambelli, A.; Allegra, G. *Macromolecules* **1980**, *13*, 42.
(17) Corradini, P.; Guerra, G.; Pucciariello, R. *Macromolecules* **1985**, *18*, 2030.

An Exact Method To Determine the Complete Orientation Distribution Function of the Chain Axis from an Arbitrary (*hkl*) Reflection†

Ravi F. Saraf

T. J. Watson Research Center, Yorktown Heights, New York 10598.
Received September 3, 1987; Revised Manuscript Received February 29, 1988

ABSTRACT: A pole inversion formula is derived for textures with an axis of symmetry, for example, planar and fiber orientation obtained by uniaxial and biaxial deformation processes, respectively. The measured pole density distribution function of an (*hkl*) reflection is expressed as an integral transform of the (required) pole density distribution function (which is usually the chain axis in polymers). Unlike other methods for pole inversion, this formulation does not involve any series expansion of the orientation functions. The integral equation is analytically solved for the special case when the (*hkl*) reflection is perpendicular to the chain axis, a common feature to most of the semicrystalline and liquid-crystalline polymers.

Introduction

The physical properties of (semicrystalline and amorphous) polymers, such as tensile modulus and strength, electrical and thermal conductivity, mass diffusion, and thermal expansivity, are dependent on chain orientation and extension. For semicrystalline polymers, a fraction of the chain (equal to the crystallinity) resides in the crystals, which are easier to orient compared to the amorphous phase. The changes in physical properties are thus dependent on the overall crystal texture. One method to tailor the crystal texture for improving a particular property in a given direction is by deformation. For example, by uniaxial extension, the tensile modulus is enhanced by 100-fold in polyethylene and[1,2] electrical conductivity is improved by 10-fold in polyacetylene at a draw ratio of ~ 3.[3] Thermal conductivity increases by 30-fold on drawing polyethylene by 32×,[4] and diffusivity of toluene in polypropylene drops by 30-fold at a draw ratio of 18.[5] However, the properties in the orthogonal directions are inferior to those in the initial, undeformed sample. A more "uniform" enhancement of properties (with some sacrifice of highest possible property enhancement) can be attained by more complex deformation geometries, such as biaxial stretching,[6-11] uniaxial compression,[12,13] planar deformation,[14,15] and combinations of various deformation geometries.[16-18]

Wide-angle X-ray diffraction (WAXD) is a suitable method for crystal texture analysis of polymers obtained by the above-mentioned deformation geometries.[19-22] The crystal texture is expressed in the form of a "pole figure". Pole figure plots represent the orientation distribution of a given (*hkl*) reflection with respect to the lab-frame. For isotropic orientation, the tip of the $\mathbf{R}(hkl)$ vector (perpendicular to the (*hkl*) plane) scribes a uniform orientation density sphere. For anisotropic orientation, a nonuniform orientation density is expected. The orientation density distribution on the sphere is represented by three projections along three orthogonal directions (usually the lab-frame axes). These three projections of the orientation sphere are called the pole figures. The tip of the $\mathbf{R}(hkl)$ vector is called the pole of the (*hkl*) reflection on the orientation sphere, and the orientation distribution is also called the pole density. Thus, for isotropic sample, the pole density is constant on the orientation sphere for any (*hkl*) reflection.

To relate the crystal texture to the modified anisotropic property, the orientation distribution of the chain axis (which is usually labeled as the c-axis in the crystal) is the

† Dedicated to Prof. Roger Porter on the occasion of his 60th birthday.

0024-9297/88/2221-2382$01.50/0

most important measurement. In other words, the pole figure of the (001) reflection is of interest. This can be directly measured by tilting the sample on a four-circle goniometer and measuring the relative intensity of the (001) reflection.[23] However, most of the polymers either have a weak (001) reflection or the reflection is absent.[24] The methods to obtain complete distribution function of a chain axis indirectly from one (or more) (*hkl*) reflection(s) (not parallel to the chain axis) are referred to as pole inversion techniques.[19,25-29] The pole inversion problem is important to obtain a structure–property relationship in semicrystalline polymers.

The crystal texture on uniaxial extension has a fiber symmetry, where the draw direction is the axis of symmetry. The crystal texture can be completely described by measuring the orientation distribution of the chain axis with respect to the draw axis. An important parameter relating the property and crystal texture in a uniaxially drawn sample is the average chain orientation distribution function, also called the Hermans orientation function.[30,31] Wilchinsky obtained a generalized formula, where the orientation function for chain axis can be calculated from the orientation functions of other measurable (*hkl*) reflections.[32,33] However, the method measures an average quantity, which may not be sufficient for understanding deformation mechanism and textures in more complex deformation processes. More general methods to obtain pole inversion involve series expansion of the measured function (i.e., the relative intensity of (*hkl*) reflection) and desired function (i.e., the pole density distribution of chain axis) (ref 34, 18, and related references). The pole density distribution function expressed in terms of a generalized spherical harmonic function (since the pole distribution function is mapped on a sphere) is related to the measured relative intensity (as a function of Euler angles) expanded as a spherical harmonic series. The coefficients of the generalized harmonic series are then determined by orthogonal property of the basis functions and the symmetry of the orientation distribution. For the uniaxial deformation case with fiber symmetry, the method was further extended to obtain an average orientation function for a general pole figure.[35] Techniques other than WAXD have also been reported in the literature. Bower obtained the average orientation distribution function by polarized Raman scattering and polarized fluorescence.[36] In principle, the complete orientation function can be obtained by the above-mentioned technique of pole inversion using series expansion; in practice, the analysis has an error due to series truncation.[35,34] The series truncation error is large for high orientation. Several (*hkl*) reflections are required for an accurate computation of the distribution function.[35,37]

In this paper, an integral equation is developed to invert the pole figure without series expansion. The assumptions on the symmetry of the chain distribution function are the same as the series expansion method. The texture assumed has the following symmetry: (i) the crystal is randomly oriented about the unique axis; (ii) the unique axis is randomly oriented about at least one of the sample axes. It must be noted that assumption ii is more general than the fiber texture obtained by uniaxial drawing. For example, in uniaxial compression, the chain is randomly oriented around the compression axis, but it is parallel to a plane rather than an axis (as in the case of uniaxial extension).

Crystal Texture Problem

Figure 1a shows a typical WAXD texture analysis, where the incident beam is along the unit vector $\hat{s}_0$ and the diffracted beam is along the unit vector $\hat{s}$ at a Bragg angle θ_B with respect to the incident beam. The Bragg angle corresponds to a reflection (*hkl*) suitable for pole figure measurement. The intensity measured along $\hat{s}$ is proportional to the number of planes perpendicular to $\hat{q} = \hat{s} - \hat{s}_0$. In a texture analysis the source (parallel to $\hat{s}_0$) and detector (parallel to $\hat{s}$) are kept stationary, implying the reciprocal vector, $\hat{q}$, is constant. The sample is rotated along the vertical axis, V, and horizontal axis, H (Figure 1a). The H axis is in the plane P defined by $\hat{s}_0 \times \hat{s}$ and perpendicular to $\hat{q}$. The V axis is perpendicular to the plane P. Let x, y, and z be the sample coordinates. The tilt angles Φ and Ψ are defined such that, at $\Phi = 0$ and $\Psi = 0$, z axis $\parallel \hat{q}$, x axis $\parallel V$ axis, and y axis $\parallel H$ axis. A complete pole figure can be obtained by tilting Φ from 0 to 2π and Ψ from $-\pi/2$ to $\pi/2$.[23] The orientation distribution of the *hkl* planes (defined by the vector $\mathbf{R}(hkl)$ perpendicular to the (*hkl*) planes) is proportional to the measured relative intensity of the (*hkl*) reflection corrected for path length and absorption. The orientation distribution function of $\mathbf{R}(hkl)$ is described with respect to Euler angles ϕ and ψ in the reciprocal space XYZ (Figure 1b). In the real space to reciprocal space transformation the directionality is preserved, therefore x axis $\parallel X$ axis, y axis $\parallel$ Y axis, and z axis $\parallel Z$ axis. Furthermore, by comparing

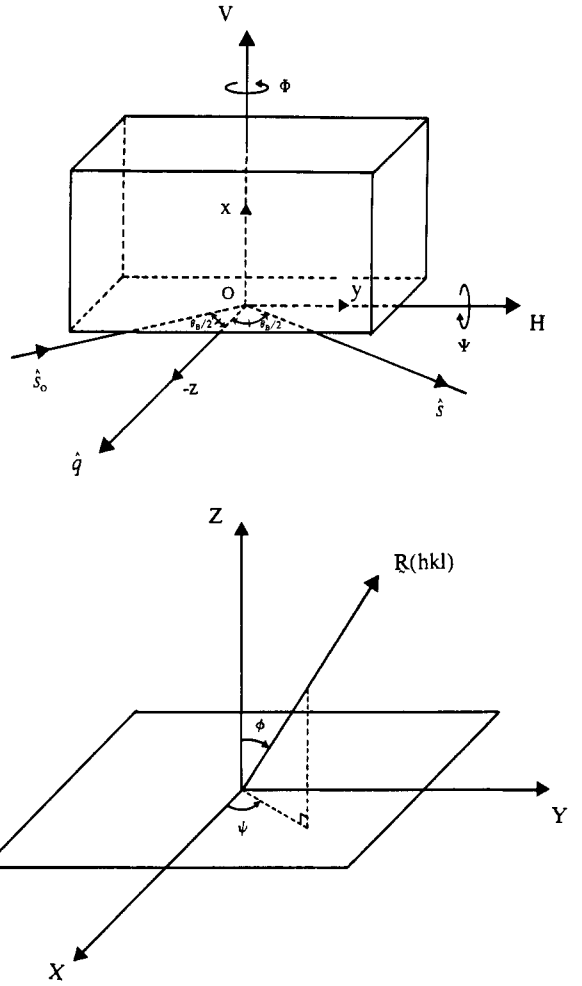

Figure 1. (a, Top) V, H, and q are the lab-frame axes. The incident beam along $\hat{s}_0$ and the diffracted beam along $\hat{s}$ are in the H–q plane. The scattering vector $\hat{q}$ is the bisector of $\hat{s}_0$ and $\hat{s}$. At tilt angles $\Phi = 0$ and $\Psi = 0$, the sample axes, x, y, and z are parallel to the V, H, and q axes, respectively. (b, Bottom) In general, for an anisotropic sample, $\mathbf{R}(hkl)$ is a function of ϕ and ψ defined with respect to the reciprocal axes, X, Y, and Z. For cylindrical symmetry, the $\mathbf{R}(hkl)$ orientation distribution is only a function of ϕ.

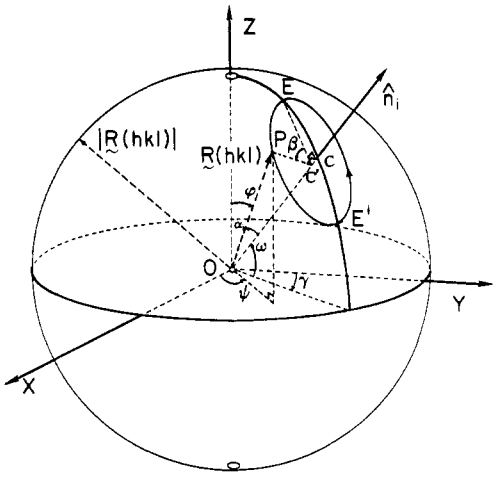

Figure 2. *O–XYZ* is the frame of reference in the reciprocal space. The unique axis $\hat{n}_i$ makes an angle ω and γ with respect to the Z and Y axes, respectively. The reciprocal lattice vector, $\mathbf{R}(hkl)$, is located by angles α_i and β with respect to the unique axis, $\hat{n}_i$. The polar coordinates of $\mathbf{R}(hkl)$ in the reciprocal space are ϕ and ψ.

parts a and b of Figure 1: at $\Psi = 0$, $\phi = \Phi$ and $\psi = \pi/2$; at $\Phi = 0$, $\phi = \Psi$ and $\psi = \pi$.

The texture for evaluation considered in this paper possesses a uniaxial symmetry, where the unique axis (usually the chain axis in polymeric materials) is randomly oriented about one of the sample axes (say, the z axis). Thus the orientation distribution is only a function of ϕ and is independent of ψ. The distribution function of (hkl) can be measured along $\Psi = 0$ or $\Phi = 0$ or a combination of the two depending on the sample geometry. Two typical cases where such a texture may occur are (i) in a uniaxially stretched sample, where the unique axis is the chain axis and the z axis is the draw direction, and (ii) in a biaxially stretched sample, where the unique axis is the chain axis and the z axis is perpendicular to the stretch plane.

Let $\hat{n}_i$ be an arbitrary direction of the unique axis at Euler angles ω and γ (Figure 2). As assumed above, the axis of symmetry is the z axis in the sample. The texture may thus be described as follows: (i) $\hat{n}_i$ is randomly oriented around the Z axis; (ii) $\mathbf{R}(hkl)$ is randomly oriented around the corresponding $\hat{n}_i$. The question is: What is the orientation distribution function of the unique axis, given the orientation distribution function of the (hkl) reflection? In other words, how does one invert the pole figure(s) of one (or more) (hkl) reflections to obtain the pole figure of the unique axis. Due to the fiber symmetry around the Z axis, the orientation distribution of $\hat{n}_i$ is independent of γ and only a function of ω. Similarly, the orientation distribution of $\mathbf{R}(hkl)$ can be described with a one-variable (or dimensional) function of ϕ. Equation 10, relating the two functions, is consistent with the mentioned symmetries.

Pole Figure Inversion

Let the unit vector along the unique axis $\hat{n}_i$ be along **OC** in Figure 2. O is the center of the orientation sphere, C lies on the surface of the sphere, and **OC** makes an angle ω with the r–θ plane. The reciprocal vector, $\mathbf{R}(hkl)$ is at an angle α_i with respect to the unique axis. Since $\mathbf{R}(hkl)$ is randomly oriented around $\hat{n}_i$, P (the tip of the vector $\mathbf{R}(hkl)$) scribes a constant pole density circle on the orientation sphere. The center of the circle C′ is in the interior of the orientation sphere.

The position of the $\mathbf{R}(hkl)$ pole is defined with respect to two sets of coordinate systems. With respect to *O–XYZ*, $\mathbf{R}(hkl)$ is located by the angles ϕ and ψ, as shown in Figure 2. With respect to the unique axis, $\hat{n}_i$, the angular coordinates for $\mathbf{R}(hkl)$ are γ and β. The angle γ locates the position of the unique axis (for a given ω) and β is defined along the circle C′ (as shown in Figure 2).

The direction of the unique axis $\hat{n}_i$ is defined by the angles, ω and γ (as shown in Figure 2). Since the crystals are randomly oriented around the Z axis, the unique axis is oriented uniformly around the Z axis. For a fixed angle, ω, **OC** will scribe a constant density circle (not shown in the Figure 2) on the orientation sphere. The center of this circle is at $Z = R \sin \omega$, where $R = |\mathbf{R}(hkl)|$. Let ρ_c be the one-dimensional (pole) density of $\hat{n}_i$ on this circle. Since the orientation is random around the Z axis, ρ_c is independent of γ and only a function of ω. The total number of $\hat{n}_i$ at a *fixed angle* ω are $q_1 = [2\pi R \cos \omega]\rho_c(\omega)$. Thus, the number of $\hat{n}_i$ on an elemental length, $R \cos \omega \, d\gamma$, is,

$$dq_1 = \rho_c R \cos \omega \, d\gamma \tag{1}$$

Let ρ be the one-dimensional (pole) density of the $\mathbf{R}(hkl)$ pole on the circle centered at C′ (as shown in Figure 2). Since the orientation of $\mathbf{R}(hkl)$ is random around $\hat{n}_i$, the density ρ is constant on the circle. For a *fixed location of the unique axis*, $\hat{n}_i(\omega,\gamma)$, the total number of $\mathbf{R}(hkl)$ planes is $q_2 = [2\pi R \sin \alpha_i]\rho(\omega)$. Thus, on an elemental length, $R \sin \alpha_i \, \beta$

$$dq_2 = \rho R \sin \alpha_i \, d\beta \tag{2}$$

For each $\hat{n}_i$ at angles ω and γ, there are q_2 number of $\mathbf{R}(hkl)$ vectors. Therefore, for dq_1 number of $\hat{n}_i$, the number of poles is $q_2 \, dq_1$. Thus, for *constant* ω, the total number of $\mathbf{R}(hkl)$ poles in an elemental length $[R \sin \alpha_i]$ $d\beta$ due to $\hat{n}_i$ in an elemental length $[R \cos \omega]$ $d\gamma$ is

$$dq = dq_1 \, dq_2 = \rho\rho_c \cos \omega \sin \alpha_i \, R^2 \, d\gamma \, d\beta \tag{3}$$

Equation 3 is the total number of $\mathbf{R}(hkl)$ in an elemental area $dA = R^2 \, d\gamma \, d\beta$ for $\hat{n}_i$ at *constant* ω and in the elemental length, $[R \cos \omega] \, d\gamma$.

The next step is to change variables from (γ,β) to spherical angles (ϕ,ψ). The experimental data are in terms of the latter angles because of the measurement optics.[23] The transformation is computed by using Figure 2 in the Appendix.

Substituting eq A8 from the Appendix into eq 3 yields the total number of $\mathbf{R}(hkl)$ poles, dq, for *constant* ω as

$$\frac{dq}{dA} = \rho_c\rho \frac{\sin \alpha_i \cos \omega}{[-\cos \phi + \sin (\alpha_i + \omega)]^{1/2}[\cos \phi + \sin (\alpha_i - \omega)]^{1/2}} \tag{4}$$

where $dA = R^2 \sin \phi \, d\phi \, d\psi$ is the elemental area on the orientation sphere. Note that the pole density, dq/dA, is not a function of ψ (as expected).

Thus, the total pole density at a given latitude, ϕ, is the sum of all the $\mathbf{R}(hkl)$ that intersect (or are tangent) to the latitude. Rigorously the summation should be over ω and γ, but integration over γ is a constant (because of the fiber symmetry). Thus, the total pole density is given as

$$\frac{dN(\phi)}{dA} = \int_{\omega_1(\phi)}^{\omega_2(\phi)} d\omega \, \frac{dq(\phi)}{dA} \tag{5}$$

where ω_1 and ω_2 are the maximum values of ω for the circle C′ to touch the (given) latitude ϕ. By simple geometry, $\omega_1 = \pi/2 - (\alpha_i + \phi)$ and $\omega_2 = \pi/2 + (\alpha_i - \phi)$. Substituting eq 4 into eq 5 yields

$$\frac{dN(\phi)}{dA} = \int_{(\pi/2)+(\alpha_i-\phi)}^{(\pi/2)-(\alpha_i+\phi)} d\omega \times \rho\rho_c \frac{\sin \alpha_i \cos \omega}{[-\cos \phi + \sin (\alpha_i + \omega)]^{1/2}[\cos \phi + \sin (\alpha_i - \omega)]^{1/2}} \quad (6)$$

Consider the physical meaning of the product $\rho\rho_c$ next. The number of $\hat{n}_i$ in a given direction defined by spherical angles ω and γ is proportional to ρ_c. The total number of $\mathbf{R}(hkl)$ is q_2 (distributed on the circle C′ in Figure 2). The corresponding $\hat{n}_i$ along this given direction is also proportional to ρ_c, because the ratio of the number of $\hat{n}_i$ planes and the (hkl) plane is a constant if the crystals are large and the crystal shape is fairly uniform over all orientations. The latter is a valid assumption in most cases. From eq 2

$$q_2 = 2\pi R \sin \alpha_i \rho \sim \rho_c$$

Since α_i and R are constants for a given (hkl) reflection

$$\rho = B\rho_c$$

where B is constant. The total number of $\hat{n}_i$ in an elemental area $(R \cos \omega)(R\, d\omega)$ is $dN_c = (\rho_c R \cos \omega\, d\gamma)(\rho_c R\, d\omega)$, since ρ_c is linear density and is constant over the arc $d\gamma$. Rearranging and replacing ρ_c^2 by $\rho_c\rho/B$ yield the total number of $\hat{n}_i$ in the elemental as

$$dN_c = \rho_c \frac{\rho}{B} R^2 \cos \omega\, d\gamma\, d\omega$$

Furthermore, due to symmetry around the Z axis, the integration over $d\gamma$ is 2π. Thus, the total number of chains is

$$dN_c = (2\pi R^2/B)\rho_c\rho \cos \omega\, d\omega \quad (7)$$

Except for the constant factor (R^2/B), $f_i(\omega) = \rho_c\rho$ is the area population density or pole density function of $\hat{n}_i$. (The proportionality constant is incorporated by proper normalization at the end of the calculation.) If $\rho\rho_c$ is replaced by the $\hat{n}_i$ pole density function $f_i(\omega)$, the above equation becomes

$$\frac{dN(\phi)}{dA} = \int_{(\pi/2)+(\alpha_i-\phi)}^{(\pi/2)-(\alpha_i+\phi)} d\omega\, f_i(\omega) \times \frac{\sin \alpha_i \cos \omega}{[-\cos \phi + \sin (\alpha_i + \omega)]^{1/2}[\cos \phi + \sin (\alpha_i - \omega)]^{1/2}} \quad (8)$$

The intensity $I(\phi)$, proportional to the total number of poles in the solid angle, $\Delta\Omega_s(\phi,\psi) = \Delta A_s/R^2$, is given by

$$I(\phi) = K'\frac{dN(\phi)}{dA}\Delta\Omega_s = K'\frac{dN(\phi)}{dA}\frac{\Delta A_s}{R^2}$$

or

$$I(\phi) = K\frac{dN(\phi)}{dA}\Delta A_s \quad (9)$$

where $\Delta\Omega_s$ and ΔA_s are the solid angle and corresponding area (on the orientation sphere) sampled in the WAXS experiment. K (or K') is a proportionality constant. The sampling size depends on instrumental parameters such as beam size and collimation, monochromaticity of the beam, and the detector (i.e., solid-state or photographic film). In the photographic film method, integrated intensity is measured. Thus, ΔA_s (or $\Delta\Omega_s$) is further modified by the Lorentz correction factor depending on the optics of the camera. No orientation angle dependent Lorentz correction is required when the sample is tilted on a four-circle goniometer, keeping the detector and source position fixed (i.e., θ_B constant), and the intensity is measured by employing a solid-state detector. For simplicity, the latter case is considered. Substituting eq 8 into eq 9 yields

$$I(\phi) = K\Delta A_s \int_{(\pi/2)-(\alpha_i+\phi)}^{(\pi/2)+(\alpha_i-\phi)} d\omega \times \frac{f_i(\omega) \cos \omega \sin \alpha_i}{[\sin \omega - \cos (\alpha_i + \phi)]^{1/2}[\cos (\alpha_i - \phi) - \sin \omega]^{1/2}} \quad (10)$$

On substituting $x = \sin \omega$

$$I(\phi) = K\Delta A_s \int_{a(\phi)=\cos(\alpha_i+\phi)}^{b(\phi)=\cos(\alpha_i-\phi)} dx \frac{f_i(x) \sin \alpha_i}{[x - a(\phi)]^{1/2}[b(\phi) - x]^{1/2}} \quad (11)$$

Equation 10 (or 11) is a Voltera integral equation of the I kind, where $I(\phi)$ is known and $f_i(\omega)$ is to be determined. Thus for a random orientation around the unique axis and fiber symmetry about the z axis, eq 10 prescribes a method to experimentally determine the orientation distribution function of the unique axis. The equation can be solved numerically to obtain $f_i(\omega)$ from the (hkl) pole figure. The integral equation can be solved exactly for special cases described below.

Solution to Integral Equation: Special Cases

The integral equation given by eq 10 or 11 can be numerically solved for a general case. However, under certain conditions the integral can be inverted analytically. The cases considered in this paper are for (i) isotropic orientation and (ii) $(hk0)$ reflection.

Isotropic Orientation. For an isotropic sample, the crystals are randomly oriented. Therefore, the pole density distribution of the chain axis is uniform over the orientation sphere, i.e., $f_i(x) = C$ (a constant). Equation 11 then leads to

$$I(\phi) = K\Delta A_s C \int_{a(\phi)=\cos(\alpha_i+\phi)}^{b(\phi)=\cos(\alpha_i-\phi)} dx \frac{\sin \alpha_i}{[x - a(\phi)]^{1/2}[b(\phi) - x]^{1/2}}$$

$$\Rightarrow I(\phi) = K\Delta A_s C \sin \alpha_i \pi \quad (12)$$

Equation 12 suggests that the intensity is independent of ϕ (as is expected for isotropic sample). Equation 12 can also be used to calculate (on a relative scale) the constants K and ΔA_s for a given polymer, provided the same optics are used to characterize the oriented and unoriented sample. Furthermore, the sample thickness and differences in crystallinity between the oriented and isotropic sample have to be corrected. The former is an absorption factor, and the latter is a multiplicative constant equal to the corresponding volume fraction. Thus quantitative comparison between samples as a function of extent of orientation can be made.

Exact Solution for $(hk0)$ Reflection. Owing to the long-chain nature, polymers in the ordered state (crystalline or liquid crystalline) pack with chains (in ordered, conformation) parallel to each other. This results in a strong reflection corresponding to lateral ordering of the chains. In most polymer crystals, the c axis is considered parallel to the chain axis; therefore, the lateral packing will correspond to $(hk0)$ reflection. In polymers such as Nylon 4, 8, and 77; polyallene; and poly(vinyl alcohol), where the b axis is parallel to the chain axis, the corresponding reflection is $(h0l)$. For either case, the reciprocal vector, $\mathbf{R}(hkl)$, is perpendicular to the unique axis, i.e., $\alpha_i = \pi/2$.

For $\alpha_i = \pi/2$, eq 11 becomes

$$I(\phi) = K\Delta A_s \int_{a(\phi)=-\sin\phi}^{b(\phi)=\sin\phi} dx \frac{f_i(x) \sin\alpha_i}{[\sin\phi + x]^{1/2}[\sin\phi - x]^{1/2}}$$

Substituting $t = \sin\phi$, $I(\phi) = I_1(t)$, and $f_i(\omega)$ as an even function (see Figure 2) into the above expression yields

$$I_1(t) = 2K\Delta A_s \int_{a(\phi)=0}^{b(\phi)=\sin\phi=t} dx \frac{f_i(x) \sin\alpha_i}{[t^2 - x^2]^{1/2}} \quad (13)$$

Equation 13 can be converted to the Abel equation by substituting $x^2 = x_1$ and $t^2 = t_1$. Thus, the integral inversion is given by[38]

$$f_i(x) = \frac{1}{\pi \sin\alpha_i K\Delta A_s} \frac{d}{dx} \int_{a(\phi)=0}^{b(\phi)=\sin\omega=x} dt \frac{tI_1(t)}{[x^2 - t^2]^{1/2}} \quad (14)$$

The complete orientation distribution function $f_i(\omega)$ can be obtained by integrating and differentiating digital data of measured intensity as a function of $\sin\phi$ (i.e., $I_1(t)$ instead of $I(\phi)$). The method derived in eq 14 has the following important features: (i) Almost all polymers have at least one ($hk0$) (or ($h0l$)) reflection for texture analysis. (ii) The method is applicable for planar and fiber textures, where the chains are parallel to a plane. (iii) Only *one* reflection is required to compute the chain axis orientation function for fiber texture unlike Wilchinsky's method.[32,33] (iv) The numerical integration of eq 14 is not straightforward due to singularity at the upper limit.

Conclusion

An integral method is developed to compute orientation distribution from digital data obtained from a diffractometer. The texture is assumed to have at least one axis of symmetry, such as fiber and planar orientation. The method has the following salient features: (i) No series expansion is required to compute the orientation distribution function. (ii) In principle, only one reflection is adequate to determine the complete distribution function of the chain axis. (iii) Quantitative texture evaluation as a function of processing condition can be performed by evaluating the optics and material constants from I versus $\sin\phi$ data for an unoriented sample. (iv) The derivation can be generalized to more complex textures by imposing γ dependence on ρ_c and (or) β dependence on ρ, implying f_i is a function of both ω and ψ. (v) A disadvantage of this method is the singular integral that will require more data points around the singularity.

Appendix: Coordinate Transformation

Any arbitrary $\mathbf{R}(hkl)$ defined on the orientation sphere can be expressed as

$$X = R \sin\phi \cos\psi; \quad Y = R \sin\phi \sin\psi; \quad Z = R \cos\phi \quad (A1)$$

where X, Y, and Z are the components in the rectilinear coordinates of $\mathbf{R}(hkl)$. By simple geometry, it can further be shown that

$$X = R \cos\alpha_i \sin\gamma \cos\omega + R \sin\alpha_i[\cos\beta \sin\omega \sin\gamma + \sin\beta \cos\gamma]$$

$$Y = R \cos\alpha_i \cos\gamma \cos\omega + R \sin\alpha_i[\cos\beta \sin\omega \cos\gamma - \sin\beta \sin\gamma]$$

$$Z = R \cos\alpha_i \sin\omega + R \sin\alpha_i \cos\beta \cos\omega \quad (A2)$$

The relation between the various angles is determined by equating the corresponding components in eq A1 and A2. Thus

$$\sin\phi \cos\psi = \cos\alpha_i \sin\gamma \cos\omega + \sin\alpha_i[\cos\beta \sin\omega \sin\gamma + \sin\beta \cos\gamma]$$

$$\sin\phi \sin\psi = \cos\alpha_i \sin\gamma \cos\omega + \sin\alpha_i[\cos\beta \sin\omega \cos\gamma - \sin\beta \sin\gamma]$$

$$\cos\phi = \cos\alpha_i \sin\omega + \sin\alpha_i \cos\beta \cos\omega \quad (A3)$$

Since ω is fixed

$$d\gamma\, d\beta = \begin{vmatrix} (\partial\gamma/\partial\phi)_\psi & (\partial\gamma/\partial\psi)_\phi \\ (\partial\beta/\partial\phi)_\psi & (\partial\beta/\partial\psi)_\phi \end{vmatrix} d\phi\, d\psi$$

From eq A3

$$(\partial\beta/\partial\psi)_\phi = 0 \quad (A4)$$

$$(\partial\gamma/\partial\psi)_\phi = -1 \quad (A5)$$

$$(\partial\beta/\partial\phi)_\psi = \frac{\sin\phi}{\sin\alpha_i \cos\omega \sin\beta} \quad (A6)$$

Therefore

$$d\gamma\, d\beta = \frac{\sin\phi}{\sin\alpha_i \cos\omega \sin\beta} d\phi\, d\psi \quad (A7)$$

Further substitution for $\sin\beta$ derived from the last expression in eq A3 and rearranging yield

$$d\gamma\, d\beta = \frac{\sin\phi}{[-\cos\phi + \sin(\alpha_i + \omega)]^{1/2}[\cos\phi + \sin(\alpha_i - \omega)]^{1/2}} d\phi\, d\psi \quad (A8)$$

References and Notes

(1) Kanamoto, T.; Tsuruta, A.; Tanaka, K.; Takeda, M.; Porter, R. S. *Polym. J.* **1983**, *15*, 327.
(2) (a) Nakanishi, M.; Tsuruta, A.; Kanamoto, T.; Tanaka, K.; Takeda, M.; Porter, R. S. Reports on Proceedings of Polymer Physics, Japan, 1985, Vol. 28, p 179. (b) Kanamoto, T.; Nakanishi, M.; Tanaka, K.; Takeda, M.; Porter, R. S. Reports on Proceedings of Polymer Physics, Japan, 1985, Vol. 29, p 185.
(3) Dark, Y. H.; Druy, M. A.; Chaing, C. K.; MacDiarmid, A. G.; Heeger, A. J.; Shirakawa, H.; Ikeda, S. *J. Polym. Sci., Polym. Lett. Ed.* **1979**, *17*, 195.
(4) Choy, C. L.; Chen, F. C.; Luk, W. H. *J. Polym. Sci., Polym. Phys. Ed.* **1980**, *18*, 1187.
(5) Choy, C. L.; Leung, W. P.; Ma, T. L. *J. Polym. Sci., Polym. Phys. Ed.* **1984**, *22*, 707.
(6) (a) Pearson, J. R. A.; Patrie, C. J. S. *J. Fluid Mech.* **1970**, *40*, 1; **1970**, *42*, 609. (b) Pearson, J. R. A.; Patrie, C. J. S. *Plast. Polym.* **1970**, *38*, 85.
(7) De Vries, A. J.; Bonnebat, C.; Beautemps, J. *J. Polym. Sci., Polym. Phys. Ed.* **1977**, *58C*, 109.
(8) Okajima, S.; Iwato, N.; Tanaka, H. *Polym. Lett. Ed.* **1971**, *9*, 797.
(9) Stephenson, S. E.; Meissner, J. *Proceedings of the VIII International Congress of Rheology*; Naples, Asterita, G., Marrucci, G., Nicolais, L., Eds.; Plenum: New York, 1980; Vol. II, pp 431.
(10) Choi, K. J.; White, J. L.; Spruiell, J. E. *J. Appl. Polym. Sci.* **1980**, *25*, 2777.
(11) Bodaghi, H.; Kitao, T.; Flood, J. E.; Fellers, J. F.; White, J. L. *Polym. Eng. Sci.* **1984**, *24*, 242.
(12) (a) Kitamura, R.; Hyon, S. H. *Die Makromol. Chem.* **1974**, *175*, 255. (b) Kitamura, R.; Chu, H.-D.; Hyon, S.-H. *Macromolecules* **1973**, *6*, 337.
(13) Saraf, R. F.; Porter, R. S. *J. Rheol.* **1987**, *31*, 59.
(14) Lin, L. S.; Chou, Y. T.; Hu, H. *J. Polym. Sci., Polym. Phys. Ed.* **1975**, *13*, 1659.
(15) Wilchinsky, Z. W. *J. Appl. Polym. Sci.* **1963**, *7*, 923.
(16) Kaito, A.; Nakayama, K.; Kanetsuna, H. *J. Appl. Polym. Sci.* **1985**, *30*, 1241.
(17) Zachariades, A. E.; Economy, J. *Polym. Eng. Sci.* **1983**, *23*, 266.
(18) Narayanan, M. J.; Magill, J. H. *J. Mat. Sci.* **1986**, *3*, 267.
(19) Bunge, H. J. *Texture analysis in Materials Science*; Butterworths: London, 1982.
(20) Quantitative Analysis of Textures: Proceedings of the International Seminar, Cracow; The Society of Polish Metallurgical

Engineers 1971; Karp, J., Gorczyca, S., Bunge, H. J., Pospiech, J., Dabrowski, W., Eds.
(21) Texture and the Properties of Materials: Proceedings of the 4th International Conference on Texture, Cambridge; The Metals Society 1975; Devis, G. J., Dillamore, I. L., Hudd, R. C., Kallend, J. S., Eds.
(22) *Texture of Materials: Proceedings of the 5th International Conference on Texture Materials*; Gottstein, G., Lücke, K., Eds; Springer-Verlag: Berlin, 1978.
(23) Alexander, L. E. *X-ray Diffraction Methods in Polymer Science*; Wiley: New York, 1969.
(24) Tadokoro, H. *Structure of Semicrystalline Polymers*; Wiley: New York, 1979.
(25) Ewald, P. P. *J. Less Common Met.* **1972**, *28*, 1.
(26) Morris, P. R. *J. Appl. Phys.* **1966**, *37*, 359.
(27) Penelle, R. Colloque Européen sur les Textures de Déformation et de Recristallisation des Métaux et leur Applications Industrielles: Proceedings of the Conference at Pont-à-Mousson; Société Francaise de Métallurgie 1973; Penelle, R., Ed.; pp 13.
(28) Krigbaum, W. R.; Balta, Y. I. *J. Phys. Chem.* **1967**, *71*, 1770.
(29) Roe, R.-J. *J. Appl. Phys.* **1966**, *37*, 2069.
(30) Stein, R. S. *Newer Methods of Polymer Characterization*; Wiley: New York, 1964; Ke, B., Ed.; pp 155.
(31) Stein, R. S. *Structure and Properties of Oriented Polymers*; Wiley: New York, 1975; Chapter 3.
(32) Wilchinsky, Z. W. *J. Appl. Phys.* **1959**, *30*, 792.
(33) Wilchinsky, Z. W. *Advances in X-Ray Analysis*; Plenum: New York, 1963; Vol. 6, pp 231.
(34) Roe, R.-J. *J. Appl. Phys.* **1965**, *36*, 2024.
(35) Roe, R.-J.; Krigbaum, W. R. *J. Chem. Phys.* **1964**, *40*, 2608.
(36) Bower, D. I. *J. Polym. Sci., Polym. Phys. Ed.* **1972**, *10*, 2135.
(37) Krigbaum, W. R.; Adachi, T.; Dawkins, J. V. *J. Chem. Phys.* **1968**, *49*, 1532.
(38) Jones, D. S. *The Theory of Generalised Functions*, 2nd ed.; Cambridge University Press: Cambridge, 1982.

Infrared Characteristic Absorption Bands of Highly Isotactic Poly(acrylonitrile)

Masatomo Minagawa,* Kazuyuki Miyano, and Masahiko Takahashi

Department of Polymer Materials Engineering, Faculty of Engineering, Yamagata University, Yonezawa 992, Japan

Fumio Yoshii

Japan Atomic Energy Research Institute, Takasaki Radiation Chemistry Research Establishment, Takasaki 370-12, Japan. *Received December 7, 1987*

ABSTRACT: The infrared (IR) absorption spectra of highly isotactic poly(acrylonitrile) (PAN) prepared by γ-ray irradiation in a urea canal complex were studied in detail and compared with those of an atactic sample. It was found that there exist in the IR spectrum characteristic bands corresponding to the isotactic configuration of PAN. These are at 1250 and 1230 cm^{-1}. The relative intensity of these bands (D_{1230}/D_{1250}) is directly proportional to the content of isotactic triad units determined by ^{13}C NMR spectra. The relationship between the intensity of IR bands and NMR isotacticity percentage in triad units was obtained quantitatively. The assignment of the IR bands is briefly discussed based on halogen substitution experiments in the solid state, etc. Other IR spectroscopic features of isotactic PAN are briefly noted.

Introduction

It is well-known that highly stereoregular poly(acrylonitrile) (PAN) can be prepared by γ-ray irradiation in a urea canal complex of acrylonitrile.[1] The stereochemical structure of PAN prepared by such a method has been assigned to be an essentially isotactic configuration.[1,2] However, little infrared (IR) spectroscopic study of stereoregular PAN has been made. In this article, some IR spectroscopic features of highly isotactic PAN are described in relation to those of radically and anionically prepared PAN. The complete assignment of the IR bands of ordinary free radical PAN has already been made by Liang and Krimm.[3,4] Here we report that careful investigation of IR spectra can reveal the configurational differences of PAN molecules through the variation of the deformation modes of methine (CH) and methylene (CH_2) groups.

Experimental Section

Sample. Isotactic PAN was prepared in the manner of White[1] and Yoshii.[5] The sample was obtained in the form of a crystalline powder. For comparison, four different types of free radical samples[6] and one kind of anionically prepared sample were also used. These are characterized in Table I.

^{13}C NMR Measurements. The JEOL NMR spectrometers JNM FX-90 Q and FX-100 were used. All the samples were measured in solution in deuteriated dimethyl sulfoxide (DMSO-d_6) at an elevated temperature. The conditions were as follows: frequency, 22.49 MHz; solvent, DMSO-d_6; concentration, 10–2%; temperature, 90 °C.

IR Measurements. The Hitachi double-beam grating IR spectrophotometers EPI-G_2 and A-285 were used. For quantitative purposes each spectrum was recorded at a sufficiently slow

Table I
Characterization of Samples

sample polymerization	code	viscosity (η)[a]	NMR results triad tacticity,[b] % I	H	S	$4IS/H^2$
canal[c]	C-1	1.61	72	22	6	3.44
canal	C-2	1.34	66	25	9	3.69
canal	C-3	1.52	67	24	9	3.99
canal	C-4	4.96	48	36	16	2.41
canal	C-5	4.58	48	35	17	2.60
anion[d]	A-1	2.17	30	43	27	1.82
radical	R-1[e]	2.14	25	51	24	0.94
radical	R-2[f]	1.97	28	46	26	1.35
radical	R-3[g]	6.03	29	49	22	1.07
radical	R-4[h]	6.87	26	47	27	1.32

[a] DMF, at 25 °C. [b] Peak intensity was calculated based on methine carbon. [c] All the canal samples were prepared by in-source method. [d] Prepared in THF by sodium–naphthalene, at −78 °C. [e] Homogeneous solution (DMSO/AIBN, at 55 °C). [f] Aqueous redox slurry (H_2O/APS-$NaHSO_3$, at 40 °C). [g] Aqueous solution (H_2O/APS, at 50 °C). [h] Bulk (photoinitiated, at 14 °C). THF, tetrahydrofuran; DMSO, dimethyl sulfoxide; AIBN, azobisisobutyronitrile; APS, ammonium peroxodisulfate.

* Author to whom correspondence should be addressed.

0024-9297/88/2221-2387$01.50/0